JOURNAL OF CATALYSIS **107**, 103–113 (1987)

# Catalytic Hydrodesulfurization over the Mo(100) Single Crystal Surface

## II. The Role of Adsorbed Sulfur and Mechanism of the Desulfurization Step

A. J. GELLMAN,[1] M. E. BUSSELL, AND G. A. SOMORJAI

*Materials and Chemical Sciences Division, Lawrence Berkeley Laboratory and Department of Chemistry, University of California, Berkeley, California 94720*

Received August 19, 1986; revised February 17, 1987

The study of thiophene hydrodesulfurization (HDS) over initially clean Mo(100) surfaces has been extended to include sulfided surfaces. Low sulfur coverages ($0 \leq \theta_S < 0.67$) inhibit HDS activity. Increasing the sulfur coverage in the range $0.67 \leq \theta_S \leq 1.0$ produces a surface with an HDS activity of about half that of the clean Mo(100) surface. Excessive exposure of the surface to a sulfur-containing environment results in the formation of a $MoS_2$ layer which is, at least in part, responsible for complete catalytic deactivation. Radiotracer ($^{35}S$) labeling techniques have been used to measure rates of hydrogenation of sulfur adsorbed on the Mo(100) surface. In ambient atmospheres of both hydrogen (1 atm) and the thiophene HDS reaction mixture ($P(H_2)$ = 1 atm, $P$(Th) = 2.5 Torr) the rate of hydrogenation of adsorbed sulfur is two orders of magnitude less than the HDS rate. This fact has been used to suggest that the desulfurization step of the reaction does not proceed via the formation of a tightly bound Mo–S species.

## I. INTRODUCTION

Preceding work has shown that Mo single crystal surfaces can be used to model and study the molybdenum sulfide-based catalysts used for the hydrodesulfurization (HDS) process (*1*, *2*). The overall mechanistic pathway is initiated by a desulfurization step leading to the formation of butadiene. Subsequent hydrogenation of an adsorbed hydrocarbon intermediate results in butene and butane production. The mechanism of the initial step is in question and it is the aim of this work to ascertain the nature of this reaction and to determine the effect of adsorbed sulfur on the activity of the catalyst.

The model most frequently proposed for the desulfurization step is that originally described by Lipsch and Schuit (*3*). Initial adsorption of the sulfur-containing organic molecule is postulated to be at an anion vacancy on the catalyst surface (in this case an oxygen or sulfur vacancy). The exact geometry and nature of the bonding is not specified although on the basis of theoretical calculations (*4*, *5*) it was suggested that thiophene should bond through the electron lone pair on the sulfur atom. On the other hand, surface science studies of molecular thiophene adsorption on Cu, Pt, and Mo surfaces point to a $\pi$-bonded configuration (*6–8*). Subsequent hydrogenation of the C–S bonds leads to production of butadiene and deposition of sulfur onto the catalyst surface. Final steps involve the hydrogenation of the adsorbed sulfur to $H_2S$ and the further hydrogenation of the hydrocarbon. It should be noted, however, that there is very little direct evidence for this mechanism other than a series of experiments using a catalyst labeled with $^{35}S$ (*9*). These showed that for the HDS reaction of dibenzothiophene over a sulfided Mo catalyst there is a labile sulfur species, present on the catalyst, that is an intermediate in the reaction leading to $H_2S$.

---

[1] Current address: Department of Chemistry, University of Illinois, Urbana, Illinois 61801.

0021-9517/87 $3.00

It is possible to envision a number of HDS mechanisms that do not proceed via the formation of an Mo–S species. Direct hydrogenation of C–S bonds to yield $H_2S$ and a surface bound hydrocarbon intermediate is one such possibility. Such a mechanism has been proposed, leading from dibenzothiophene to mercaptobiphenyl which is then hydrogenated to biphenyl and $H_2S$ (*10*). In the case of thiophene HDS, a mechanism has been proposed similar to that of an alcohol dehydration reaction, in which the desulfurization occurs by an intramolecular hydrogenation of the sulfur atom, leaving diacetylene as the hydrocarbon product (*11*). Investigations of the HDS of thiophene in $D_2$ showed that the sulfur-containing product was $H_2S$ rather than $D_2S$, in direct agreement with this mechanism (*12*). Such a reaction does not require the formation of a metal–sulfur bond but is impossible in the case dibenzothiophene.

This study extends the investigation of the catalytic activity of Mo(100) single crystal surfaces to study the effect of adsorbed sulfur. We have measured the rate of thiophene HDS as a function of sulfur coverage and the stability of adsorbed sulfur under reaction conditions. Using a $^{35}S$ isotope we have been able to make direct measurements of the rate of sulfur removal from the metal surface during exposure to either $H_2$ or the reaction mixture. Periodic removal of the crystal from the reaction environment allows determination of the amount of $^{35}S$ remaining on the surface by monitoring of its $\beta^-$ emission. Using this approach it is possible to discriminate between sulfur that has been deposited directly on the metal surface under ultrahigh vacuum (UHV) conditions and sulfur that has been deposited in the form of adsorbed thiophene or via the decomposition of thiophene under reaction conditions.

## 2. EXPERIMENTAL

The surface analysis chamber and methods used to perform high-pressure catalytic reactions have been described in the previous paper of this pair.

In addition to the equipment described previously, a solid-state $\beta^-$ detector was installed specifically for this work. The details of its operating characteristics and the data collection system have been described elsewhere (*15*). Briefly, the detector consists of an *n*-type silicon wafer with a 300-$\mu$m-thick depletion region. A potential of 100 V is applied across the silicon wafer via thin film gold contacts on either side of the wafer. High-energy electrons impinging on the silicon wafer create free charge carriers that are separated by the potential bias and measured as a current pulse at the contacts. The amplitude of the current pulse is proportional to the energy of the impinging electrons. The detector is held in a rotatable mount, allowing it to be directed away from the crystal when the crystal is exposed to $C^{35}S_2$ and during atmospheric pressure reactions. The detector mount was attached to a liquid nitrogen reservoir via copper braids. During operation, the detector was cooled to approximately −35°C in order to minimize the dark current.

Beta emission from the $^{35}S$ adsorbed on the Mo(100) surface was measured by rotating the detector so that it faced the center of the crystal. The crystal was then moved up to a position approximately 2 mm from the front face of the detector. The detecting surface is 8 mm in diameter and is smaller than the single crystal which has a diameter of 10 mm. Furthermore, the detecting surface is recessed by 2 mm into the detector unit itself, resulting in a geometry in which the detecting surface is quite well screened from all surfaces other than the one under study.

The background $\beta^-$ emission from the support rods could be estimated quite simply by first adsorbing a saturation amount of sulfur on the sample and then cleaning it by heating to 1600°C. The sample was mounted between two thick (0.125-in.-diam.) tantalum support rods and was attached to these via two small tantalum wires (0.02-in. diam. × 0.05 in.). Thermal insulation from the thick support rods was such that they did not heat to more than 600°C while heating the sample to 1600°C. At these temperatures sulfur will not desorb from the tantalum supports. The supports were observed to contribute a background count rate of 300–400 cpm which was subtracted from the total count rate to determine the contribution from sulfur adsorbed to the Mo(100) surface. The background represents about 25% of the total measured count rate. The tantalum supports became saturated with sulfur within a couple exposures of the crystal to the $C^{35}S_2$ after which the background current remained constant.

$^{35}S$ deposition was accomplished by decomposition of labeled $C^{35}S_2$. The labeled compound was obtained from New England Nuclear Corp. at an initial activity of 100 mCi/mmole ($^{35}S$ half-life = 87.9 days) and a radiochemical purity of better than 99%. The material was stored in a breakseal tube with a Teflon stopcock. The crystal was exposed to the $C^{35}S_2$ vapor via a doser attached to a leak valve. Use of the doser allowed exposure of the crystal while minimizing the exposure of the remainder of the chamber to $C^{35}S_2$. Sulfur overlayers were produced by exposure of the crystal to $C^{35}S_2$ followed by annealing to 800–1000°C. Heating of the crystal serves to dissociate the $C^{35}S_2$ and causes the carbon to dissolve into the bulk of the sample. In general heating a Mo crystal will cause segregation of carbon to the clean surface; however, in the presence of surface sulfur, carbon dissolves into the crystal bulk. A similar effect was reported in the case of nickel in which surface sulfur alters the thermodynamics of carbon segregation (*16*). Two or three such treatments with exposures totalling approximately $45 \times 10^{-9}$ Torr sec were sufficient to produce a sulfur overlayer at a coverage of $\theta_S = 0.75$ in a $c(4 \times 2)$ structure identical to that produced using exposures to either $H_2S$ or $S_2$. It was not possible, however, to produce overlayers of higher coverage using this approach. The calibration of AES signal and LEED patterns versus sulfur coverage on the Mo(100) surface has been discussed elsewhere (*8, 17*).

The procedure used in performing this set of experiments began with cleaning of the surface by flashing to 1600°C followed by a measurement of the $\beta^-$ emission from the clean surface to determine the background count of the sample holder. The surface was sulfided with labeled $^{35}S$ and the coverage determined. The coverage was determined with the aid of AES, LEED, and $\beta^-$ emission measurements. The sulfided surface was enclosed in the isolation cell which was then pressurized with either $H_2$ or a mixture of $H_2$ and thiophene. In the cases in which mixtures were used the gases were circulated through a batch reactor loop for approximately 30 min to ensure mixing of the gases before heating the crystal. The reactor loop was made of $\frac{1}{4}$-in. stainless-steel and was attached with both an inlet and an outlet to the cell. After mixing was complete the crystal was heated resistively to the desired temperature, usually for a period of 5 min. The temperature was maintained by a controller which monitored the potential across the Pt–Pt/Rh 10% thermocouple attached to the crystal. After heating, the crystal was allowed to cool in the gas mixture which was then pumped out of the cell using a mechanical pump followed by an oil diffusion pump. In the case of a pure hydrogen atmosphere the cell was evacuated for 15 min while on the occasions in which a hydrogen/thiophene mixture was used, the evacuation time was about 2 hr. The cell was then opened exposing the crystal to ultrahigh vacuum conditions and a measurement was made of the $\beta^-$ emission from the surface to determine the coverage of $^{35}S$ remaining on the surface. The procedure was repeated using either the existing surface or a freshly prepared surface as necessary.

## 3. RESULTS

### 3.1. *The Effect of Adsorbed Sulfur on Thiophene HDS*

Figure 1A depicts the rate of thiophene hydrodesulfurization over the Mo(100) surface as a function of sulfur coverage. The initial sulfiding of the surface, under UHV conditions, prior to the reaction resulted in a decrease in activity at low coverages which continued to decrease up to a coverage of approximately 0.6, beyond which the further addition of sulfur had very little effect. The activity of the surface at these coverages was reduced to almost half that of the clean surface. The fact that the addition of sulfur to the surface can inhibit the reaction suggests that this adsorbed sulfur species remains on the surface during the reaction and thus cannot be an intermediate species in the reaction mechanism. It is also interesting to note in Fig. 1B that the HDS reaction products are not uniformly affected by the presence of sulfur. While the rates of butene and butane production follow the behavior described above, the rate of butadiene production is virtually unaffected by adsorbed sulfur.

The inhibition of the reaction rate at low coverages is caused by sulfur atoms adsorbed in fourfold hollow sites on the surface (*8*). This sulfur must remain adsorbed on the surface during the reaction. At high coverages ($\theta_S > 0.67$) the sulfur atom is adsorbed in a second, less tightly binding site (*8*). The fact that the addition of sulfur to the surface at these high coverages has little additional effect on the reaction rate suggests that the sulfur in this second binding site is easily reduced and that removal of sulfur from this site is relatively fast. This implies that a reaction that is initiated on a metal surface that is initially covered with one monolayer of sulfur results in an immediate reduction of this coverage to the point at which only hollow sites are occupied. Immediate reduction implies a reaction that is fast on the time scale by which HDS rates are measured (~15 min).

### 3.2. *Deactivation of the Mo(100) Catalyst*

Extended exposure of the Mo(100) surface to the HDS reaction mixture resulted in a very high surface sulfur coverage that was accompanied by formation of a $MoS_2$ compound overlayer and a lower HDS ac-

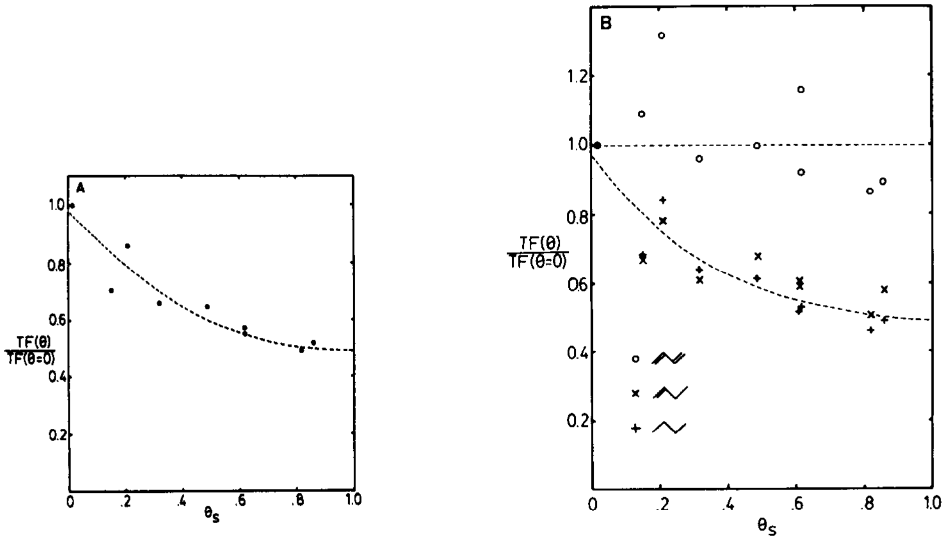

FIG. 1. (A) Rate of thiophene HDS vs initial sulfur coverage of the Mo(100) surface. Rates are given relative to those on the clean surface. $P(H_2)$ = 780 Torr, $P$(Th) = 2.5 Torr, $T$ = 340°C. (B) Rates of butadiene, butene, and butane production vs $\theta_S$. Rates are relative to those on the clean surface.

tivity. This is a process that is distinct from the inhibition of activity by sulfur preadsorbed under UHV conditions in that it involves the formation of a $MoS_2$ compound overlayer.

After a period of steady-state activity of about 90 min, the reaction rate over the single crystal surface begins to fall until, after ~12 hr there is no further activity under our experimental conditions. Although turnover numbers at this point are in excess of 1500 the total conversion of reactants is <15%. The long-term deactivation of the catalytic surface has not been investigated thoroughly as yet but several possible causes exist. Competition for reactant adsorption sites by the $H_2S$ product has been observed over dispersed catalysts. In our batch reactor this could lead ultimately to the complete deactivation of the catalyst as the $H_2S$ partial pressure is continuously increasing. A second effect that may lead to catalyst deactivation is the growth of a $MoS_2$ overlayer oriented to expose its inactive basal plane. A typical AES spectrum of the crystal surface after a long reaction time yields a $S_{150}:Mo_{221}$ AES ratio that approaches the value of ~12 : 1 observed for a $MoS_2$ single crystal (*13*). In general no LEED pattern can be observed from the surface unless the duration of the reaction is fairly short, in which case the sulfur coverage is less than a monolayer and a square lattice due to diffraction from the Mo(100) substrate can be observed.

Annealing of a heavily sulfided surface to 800–1100°K will produce the LEED pattern shown in Ref. (*2*) with no significant change in the AES spectrum. This LEED pattern has diffraction spots forming a square lattice, again produced by the substrate, and a circle of diffraction intensity with 12 maxima around its perimeter. These are due to diffraction from two domains of a hexagonal overlayer rotated at 30° with respect to each other. The lattice spacing of this hexagonal overlayer is 3.11 ± 0.05 Å which is almost identical to that of $MoS_2$ (3.15 Å) (*14*). This sulfide structure has been grown on both the Mo(100) and Mo(111) surfaces by exposures to $H_2S$ (~1 Torr) at high temperatures (>500°C) and has been determined to be the basal plane of $MoS_2$. This assessment has been made based upon the above observations and the comparison of electron energy loss (ELS) and LEED I/V measurements with those made on bulk $MoS_2$ (*21–23*). On occasion this structure has been observed immediately following a HDS reaction without the need for annealing. This suggests that after long reactions (12 hours), the surface is composed of a $MoS_2$ overlayer having a high $S_{150}:Mo_{221}$ AES ratio but not sufficiently well ordered to produce a LEED pattern. The effect of annealing is to induce long range order. Deactivation of the Mo(100) catalyst apparently occurs by reversible adsorption of $H_2S$ onto active HDS sites and by formation of the inactive $MoS_2$ basal plane at the surface of the single crystal.

### 3.3. Mo(100)–$^{35}S$ Reduction in $H_2$

The $^{35}S$ overlayer on the Mo(100) surface produced a $\beta^-$ emission signal of approximately 1800 counts per minute (cpm) at a coverage of $\theta_S = 0.75$ on initial receipt of the $C^{35}S_2$. Exposure of the surface to $H_2$ (1 atm) at 340°C for 5 min results in no measurable loss of $^{35}S$ from the surface. Figure 2 shows the loss of $^{35}S$ from the surface at a temperature of 525°C. A fit to a first-order kinetic equation

$$r = \frac{d\theta_S}{dt} = k\theta_S$$

yields the rate constant for removal, $k = 3.0 \times 10^{-4}$ $site^{-1}$ $sec^{-1}$. Note that this rate constant contains no dependence on $\theta_H$, and even at this temperature it is less than the measured rate of thiophene HDS at 340°C of 0.11 molecule $site^{-1}$ $sec^{-1}$. Kinetic measurements of the rate of sulfur removal give an activation energy of 13.9 kcal/mole in the temperature range 400–550°C, and an order in hydrogen pressure of 0.34 over the pressure range 50–780 Torr (Figs. 3 and 4).

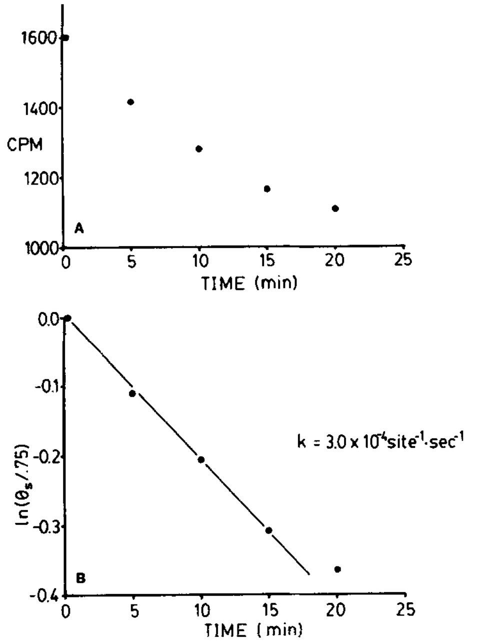

FIG. 2. (A) Decrease in $^{35}S$ signal with time during reduction in $H_2$. Initial coverage was $\theta_S = 0.75$, $T = 525°C$, $P(H_2) = 780$ Torr. (B) Plot of $\ln(\theta_S/0.75)$ vs $t$ shows first-order kinetics.

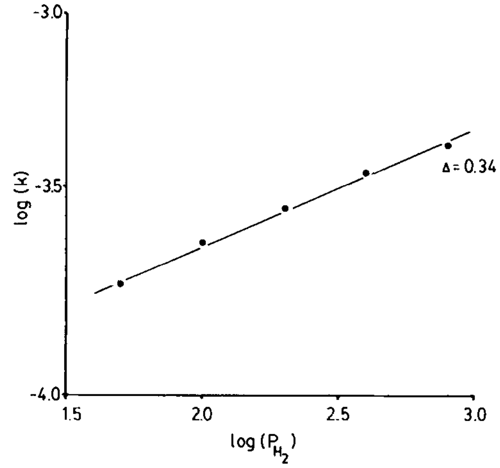

FIG. 4. Order plot of the rate constant for sulfur removal vs hydrogen pressure. $T = 550°C$.

Extrapolation of the Arrhenius plot to 340°C yields a rate of approximately $2 \times 10^{-5}$ $sec^{-1}$, about four orders of magnitude less than the observed HDS rate of thiophene. The reduction of sulfur, bound to the metal surface, by hydrogen is clearly not a step that is involved in the HDS of thiophene.

The rate of sulfur removal from the surface was measured at several initial sulfur coverages (Fig. 5). Although the rate was measurable at 500°C for coverages of 0.75,

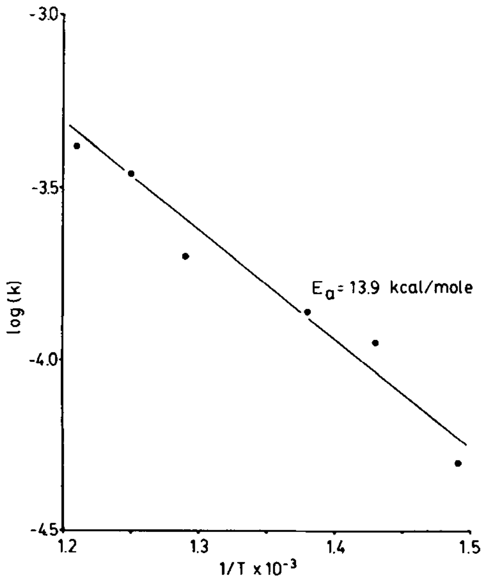

FIG. 3. Arrhenius plot of the rate constant for sulfur removal in hydrogen. $P(H_2) = 780$ Torr.

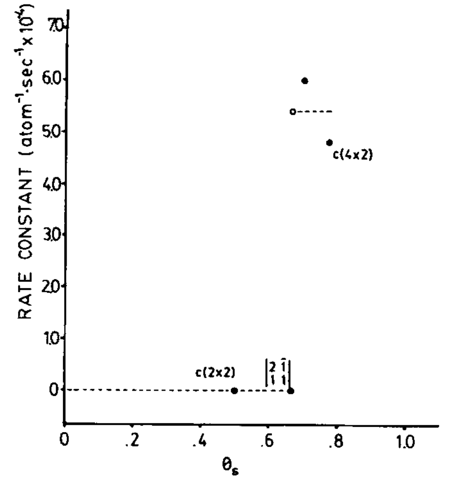

FIG. 5. Rate constant for sulfur removal vs sulfur coverage. Reaction times were limited to 5 min to minimize the effects of contamination by background hydrocarbons. $T = 500°C$, $P(H_2) = 780$ Torr. The detection limit for sulfur removal rate constant was $2 \times 10^{-5}$ $atom^{-1}$ $sec^{-1}$.

at coverages of $\theta_S \leq 0.67$ there was no measurable reduction in the $^{35}S$ signal after treatment with $H_2$ for 5 min. Repetitive exposures would result in the buildup of contaminant sulfur and carbon from the reaction loop and the displacement of sulfur. It is interesting to note that the coverage at which it becomes impossible to remove the sulfur is $\theta_S = 0.67$. It is at this coverage that the sulfur atoms begin to populate the high coverage binding site rather than the fourfold hollow sites (*8*).

### *3.4. Mo(100)–S Reduction under HDS Conditions*

In addition to studying the reduction of sulfur overlayers in $H_2$, similar measurements have been carried out in the presence of the HDS reaction mixture. The kinetic measurements show that the reaction is much different from that in pure $H_2$ (Figs. 6–8). The most pronounced effect of the addition of thiophene to the reaction mixture is a marked increase in the rate of sulfur removal. Under the conditions of $T = 345°C$, $P(H_2) = 780$ Torr, and $P(Th) = 1$ Torr, very close to those used to study the HDS reaction, the removal rate constant is $6.8 \times 10^{-4}$ sec$^{-1}$, 30 times greater than that observed in pure $H_2$, but still two orders of magnitude lower than the observed thiophene HDS rate.

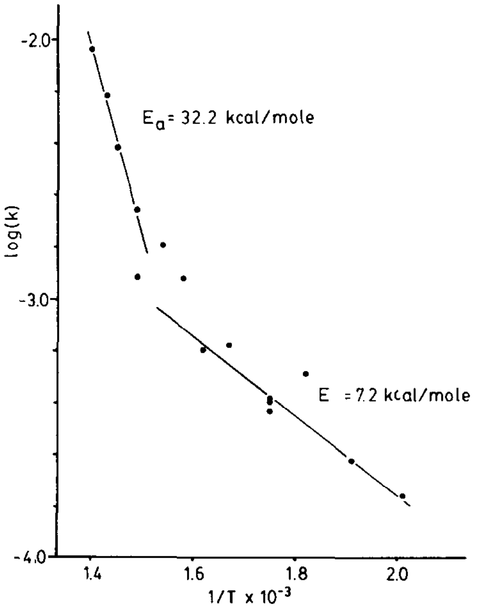

FIG. 6. Arrhenius plots of rate constants for sulfur removal in both thiophene and hydrogen. $P(Th) = 1.0$ Torr, $P(H_2) = 780$ Torr.

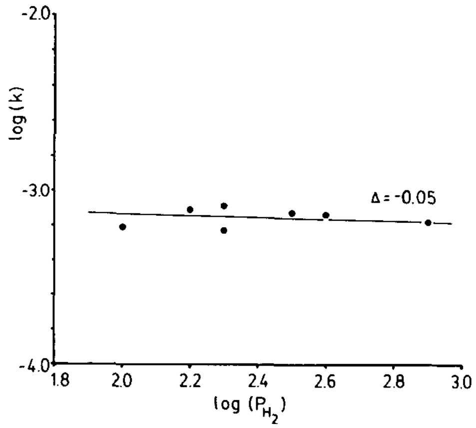

FIG. 7. Order plot of the rate constant for sulfur removal vs hydrogen pressure. $P(Th) = 1.00$ Torr, $T = 345°C$.

An Arrhenius plot of the rate over a temperature range of 225–440°C shows a distinct break at approximately 380°C with a change of activation energy from 7.2 kcal/mole in the low-temperature regime to 32.2 kcal/mole in the high-temperature regime. The sulfur removal rate has been measured at 325°C, in the low-temperature

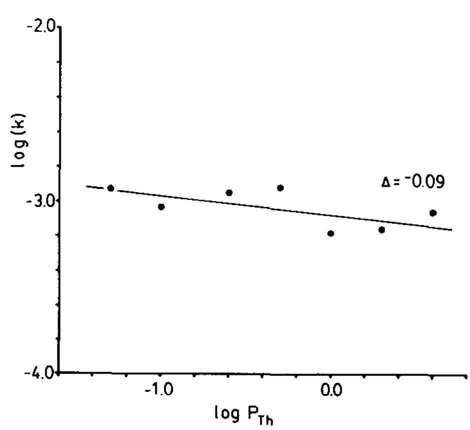

FIG. 8. Order plot of the rate constant for sulfur removal vs thiophene pressure. $P(H_2) = 780$ Torr, $T = 345°C$.

regime, over a range of reactant concentrations and been shown to be independent of both thiophene and hydrogen pressures. This is true even for very low concentrations of thiophene ($<10^{-3}$ Torr). After performing reactions with thiophene it was necessary to flush the reaction loop with $H_2$ for several hours before measuring sulfur removal rates characteristic of those in pure $H_2$.

There was no significant difference in rates between surfaces starting with $\theta_S = 0.5$ and 0.75 as was observed in the case of pure $H_2$. In the cases in which thiophene was included in the reactant mixture even sulfur atoms bound in the fourfold hollow sites could be displaced, although their residence time on the surface was still very long, i.e., approximately 30 min. The sulfur deposited on the surface before an HDS reaction remains on the surface for periods of time much longer than the residence times of either reactants or products.

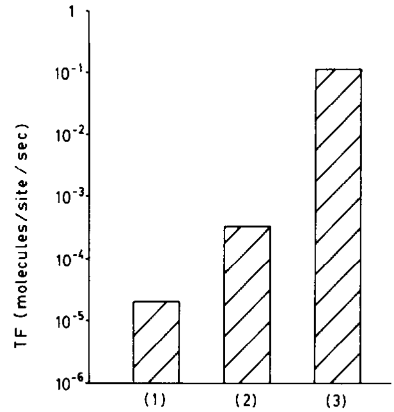

FIG. 9. Relative rates of thiophene HDS (3), sulfur hydrogenation in a pure $H_2$ environment (1), and sulfur hydrogenation in a thiophene/$H_2$ atmosphere (2) on the Mo(100) surface. $P(H_2) = 780$ Torr, $P(\mathrm{Th}) = 2.5$ Torr, $T = 340°\mathrm{C}$.

## 4. DISCUSSION

The implications of the results of this study for HDS catalysis can be understood by comparing the rates of sulfur removal from the Mo(100) surface and of thiophene HDS over these surfaces. The rate of hydrogenation of adsorbed sulfur to $H_2S$ is much slower than the rate of hydrodesulfurization under the same conditions. The rates of these processes, under comparable conditions are depicted in Fig. 9. These findings eliminate the Lipsch–Schuit mechanism of desulfurization (depicted in Fig. 10A) in which the sulfur is first adsorbed onto the catalyst as a result of hydrogenolysis of C–S bonds and is subsequently hydrogenated. In this circumstance, the sulfur hydrogenation reaction would be rate-limiting, and the HDS reaction rates would be much slower than those observed. It is not, of course, possible to rule out a mechanism in which the sulfur atom is deposited onto the surface in a very weakly bound state (Fig. 10B) from which it is easily reduced. The nature of such a state, however, would be much different from any observed during the adsorption of sulfur on the Mo(100) surface under UHV conditions (i.e., the Mo–S bond strength must be $\leqslant 75$ kcal/mole). Its bonding to the metal must be sufficiently weak that reduction to $H_2S$ is much faster than any exchange reaction with sulfur bound directly to the metal. It is difficult to understand what the driving force would be for the breaking of C–S bonds to form such a species. Instead, the desulfurization step must be one in which $H_2S$ is produced without the formation of an adsorbed sulfur atom (Fig. 10C).

The kinetic studies of thiophene HDS have shown that the initial steps to produce butadiene are independent of hydrogen pressure and first order in thiophene pressure. This has been discussed in terms of a rate-determining step that occurs prior to any hydrogenation steps. The fact that butene production is fractional order in hydrogen pressure has suggested that the hydrogen coverage is low and the first-order dependence in thiophene pressure rules out a mechanism in which one of the hydrocarbon intermediates leading to butadiene is saturating the surface. Finally, the activation energy of the rate-determining step has been found to be approximately 14 kcal/mole. Two mechanisms for

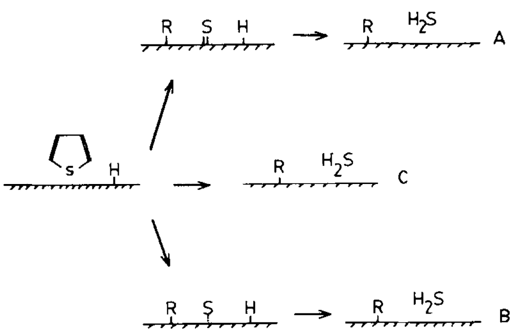

FIG. 10. Possible mechanisms for the initial desulfurization of thiophene. (A) The Lipsch–Schuit mechanism involving deposition of sulfur onto the catalyst followed by reduction by surface hydrogen. (B) Deposition of sulfur into a weakly bound adsorption state followed by hydrogenation. (C) Direct extrusion of sulfur from the thiophene ring to form $H_2S$ without the intermediate formation of an Mo–S species.

the initial desulfurization step are consistent with the observations of this work. One would lead to a reaction in which hydrogenolysis of C–S bonds by adsorbed hydrogen proceeds without the intermediate formation of an Mo–S bond, yielding $H_2S$ and an adsorbed hydrocarbon intermediate that is readily reduced to butadiene. In this case the rate-determining step is one occurring prior to the hydrogenolysis step, either the adsorption of thiophene or the production of some activated adsorption state in which the hydrogenolysis can occur. It is unlikely that simple chemisorption is activated. However, studies of thiophene chemisorption on the Mo(100) surface (*8*) showed the existence of a molecular adsorption state, stable to high temperatures (>450°K), that was produced only upon heating to approximately 200°K (i.e., activated). Although no direct correlation to the high-pressure reaction can be made, such a species might be hydrogenated at high pressures to yield the HDS products. The second mechanism that is consistent with the current work is that proposed by Kolboe (*11*), which is a dehydrodesulfurization reaction. The production of $H_2S$ occurs intramolecularly leading to adsorbed diacetylene. It seems reasonable to suggest that such an initial step would be activated and might be rate-limiting. Furthermore the hydrogenation of diacetylene to butadiene would be expected to be very fast (*19*). Such a mechanism would not be possible in the case of dibenzothiophene, but labeling studies of the HDS of this compound show that it does proceed by a Lipsch–Schuit type mechanism (*9*) (as in Fig. 10A).

The measurements of sulfur hydrogenation in $H_2$ show that the hydrogenation of the high coverage sulfur species is faster than that of the low coverage species ($\theta_S > 0.67$). This was predicted from the study of the rates of thiophene HDS reactions at various different initial sulfur coverages in which the low coverage sulfur was found to have a strong inhibiting effect, while increasing the coverage caused little additional change. Previous work has shown that at high coverages the Mo(100)–S bond strength is 75–90 kcal/mole, reduced from its low coverage value of 110 kcal/mole (*24*). The suggestion is that this weakly bound sulfur species may be readily reduced to $H_2S$ and thus has little effect on the HDS activity. Calculations of the equilibrium coverages of sulfur in $H_2$ (1 atm, 340°C), using 110 and 80 kcal/mole, respectively, for the two Mo–S species, show that the steady-state coverage of the tightly bound species is almost unity while that of the weakly bound species is approximately $5 \times 10^{-4}$. The coverage at which sulfur can be reduced is that at which the high coverage binding site, postulated to be a bridging site, becomes postulated. The present results provide further evidence that there is some change in the bonding of sulfur to the surface on going from the $\left[\begin{smallmatrix}2 & \bar{1}\\ 1 & 1\end{smallmatrix}\right]$ ($\theta_S = 0.67$) structure to the $c(4 \times 2)$ ($\theta_S = 0.75$) structure.

The details of the mechanism by which preadsorbed sulfur determines the reaction rate are unclear. In the presence of thiophene all of the $^{35}S$ can be reduced from the metal surface, but on a time scale that is much longer than the reaction rate. The preadsorbed sulfur selectively inhibits the hydrogenation reactions leading to the butenes and butane, but not the desulfurization reaction leading to butadiene. Kinetic studies suggest that the hydrogenated products are formed via a partially hydrogenated intermediate that saturates its available binding sites on the surface, thus leading to the very weak dependence of the rates of butene and butane production on thiophene pressure. The presence of preadsorbed sulfur blocks binding sites for such an intermediate. The simplest explanation for the shape of the rate versus $\theta_S$ curve would be that sulfur adsorbed in the fourfold hollow sites ($\theta_S \leq 0.67$) remains on the surface permanently, blocking adsorption sites for the intermediate leading to the hydrogenated products. Sulfur adsorbed on the surface at coverages greater than 0.67 is present in the high coverage binding site and is reduced from the surface very quickly, and thus has no effect on the reaction rate. Such an ideal situation would be expected to result in a linear decrease of the rate in the coverage regime $0 < \theta_S < 0.67$, and for $\theta_S \geq 0.67$, a rate equal to that at $\theta_S = 0.67$. While the results presented here approximate such a process, the situation is clearly much more complicated due to the fact that the removal of sulfur from the high coverage sites is not infinitely fast, nor is the removal rate of sulfur from the low coverage sites equal to zero. Furthermore, in the presence of thiophene there is some deposition of sulfur onto the surface, albeit at a rate much less than that of the reaction.

The sulfur reaction kinetics in pure hydrogen can be modeled by a simple scheme of hydrogen adsorption followed by a sequential hydrogenation of sulfur atoms and, finally, desorption of $H_2S$.

$$\begin{aligned} H_2(g) &\rightarrow 2H(ads) \\ S + H(ads) &\rightarrow SH \\ SH + H(ads) &\rightarrow SH_2 \\ SH_2 &\rightarrow H_2S(g) \end{aligned}$$

The fact that the hydrogen pressure dependence is not one-half order indicates that the first step of hydrogen adsorption is not rate-limiting. Unfortunately, it was not possible to cover a great enough range of hydrogen pressures to allow determination of which step among the remainder is rate-limiting.

The final point of interest in this study is the dramatic influence of thiophene on the rate of sulfur reduction. Very low pressures of thiophene resulted in an enhancement of the reduction rate by more than an order of magnitude. The rate increase may be caused by a change in the metal–sulfur bonding due to the presence of coadsorbed thiophene or by a change of reaction mechanism.

The reduction of sulfur in pure $H_2$ has been noted to occur at a faster rate as the Mo–S bond is weakened on increasing the coverage past 0.67 monolayers. This bond weakening is due to the change in the sulfur adsorption site with coverage, induced by repulsive interactions between adsorbed sulfur atoms. If such an effect were produced by the presence of thiophene, a similar increase in the reaction rate would be expected. Such an effect, however, would be expected to manifest itself in a decrease in the reaction activation energy. At temperatures of 390–440°C this is clearly not the case as the apparent activation energy increases from 14 to 32 kcal/mole on introducing thiophene. In the lower temperature range, outside that accessible when working with pure $H_2$, the activation energy is lowered by the presence of thiophene. The preexponential factor and the kinetics, however, are also different, suggesting a new sulfur removal mechanism.

It is interesting to note that the removal rate of sulfur in the HDS mixture is independent of both thiophene and hydrogen pressures. Studies of the HDS kinetics point to the existence of a hydrocarbon intermediate that is saturating the surface and is in equilibrium with adsorbed hydrogen. Its concentration is independent of both thiophene and hydrogen pressures. It is possible that such a species serves as a source of hydrogen for sulfur removal, accounting both for the enhancement in the reaction rate and the change in the observed kinetic parameters. The presence of a carbonaceous deposit serving as a source of hydrogen during hydrogenation reactions has been discussed elsewhere (*20*). In the case of ethylene hydrogenation over Pt(111) and Rh(111) surfaces, such deposits have been identified as ethylidyne moieties (*2, 18*). In this case, however, the nature of such a species is unknown and should be the subject of further investigation.

## 5. CONCLUSION

The primary mechanistic implication of this work on thiophene hydrodesulfurization over Mo(100) single crystal surfaces is that the desulfurization step does not occur via the Lipsch–Schuit mechanism. Carbon–sulfur bonds are not broken to form an intermediate metal sulfur species such as is observed during sulfur adsorption on the Mo(100) surface under UHV. These sulfur species have high heats of adsorption (75 kcal/mole) and if formed their hydrogenation to $H_2S$ would be reaction rate-limiting (Fig. 10A). It is possible that a weakly adsorbed intermediate is produced (Fig. 10B) but it should be noted that its rate of hydrogenation must be much greater than any interconversion with the tightly bound species. Instead, we suggest that the desulfurization step occurs via either the Kolboe mechanism of intramolecular dehydrodesulfurization or a direct hydrogenolysis of C–S bonds to form $H_2S$ (Fig. 10C).

Measurements of the rate of hydrogenation of surface sulfur in 1 atm of pure $H_2$ at various sulfur coverages show a discontinuity as the coverage exceeds $\theta_S = 0.67$. At the lower coverages the rate is below the detection limits of the experiment, while for $\theta_S > 0.67$ it is quite significant but still two orders of magnitude lower than the rate of HDS of thiophene. This result points to a distinct change in the Mo(100)–S bonding at this coverage. It supports the suggestion made previously that it is at this coverage that adsorbed sulfur atoms begin to occupy a weakly binding site different from the fourfold hollow site occupied at $\theta_S \leq 0.5$.

## ACKNOWLEDGMENTS

This work was supported by the Director, Office of Energy Research, Office of Basic Energy Sciences, Materials Sciences Division of the U.S. Department of Energy under Contract DE-AC03-76SF00098.

## REFERENCES

1. Gellman, A. J., Farias, M. H., and Somorjai, G. A., *J. Catal.* **88,** 546 (1984).
2. Gellman, A. J., Neiman, D., and Somorjai, G. A., *J. Catal.* **107,** 92 (1987).
3. Lipsch, J. G., and Schuit, G. L. A., *J. Catal.* **15,** 179 (1969).
4. Duben, A. J. J., *Phys. Chem.* **82,** 348 (1978).
5. Harris, S., and Chianelli, R. R., *J. Catal.* **86,** 400 (1984).
6. Richardson, N. V., and Campuzano, J. C., *Vacuum* **31,** 449 (1981).
7. Stohr, J., Gland, J. L., Kollin, E. B., Koestner, R. J., Johnson, A. L., Muetteries, E. L., and Sette, F., *Phys. Rev. Lett.* **53,** 2161 (1984).
8. Gellman, A. J., Tysoe, W. T., and Somorjai, G. A., to be published.
9. Gachet, C. G., Dhainaut, E., de Mourgues, L., Candy, J. P., and Fouillous, P., *Bull. Soc. Chim. Belg.* **90,** 1279 (1981).
10. Singhal, G. H., Espino, R. L., and Sobel, J. E., *J. Catal.* **67,** 446 (1981).
11. Kolboe, S., *Canad. J. Chem.* **47,** 352 (1969).
12. Mikovsky, R. J., Silvestri, A. J., and Heinemann, H., *J. Catal.* **34,** 324 (1974).
13. Salmeron, M., Somorjai, G. A., Wold, A., Chianelli, R. R., and Liang, K. S., *Chem. Phys. Lett.* **90,** 105 (1982).
14. Wilson, J. A., and Yoffe, A. D., *Adv. Phys.* **18,** 193 (1969).
15. Davis, S. M., Gordon, B. E., Press, M., and Somorjai, G. A., *J. Vac. Sci. Technol.* **19,** 231 (1981).
16. Ramanathan, R., Quinlan M., and Wise, H., *Chem. Phys. Lett.* **106,** 87 (1984).
17. Maurice, V., Peralta, L., Beathier, Y., and Oudar, J., *Surf. Sci.* **148,** 623 (1984).
18. Zaera, F., Ph.D. thesis, University of California, Berkeley, 1984.
19. Gates, B. C., Katzer, J. R., and Schuit, G. C. A., "Chemistry of Catalytic Processes," p. 263. McGraw–Hill, New York, 1979.
20. Davis, S. M., Ph.D. thesis, University of California, Berkeley, 1981.
21. Wilson, J. M., *Surf. Sci.* **53,** 330 (1975).
22. Wilson, J. M., *Surf. Sci.* **55,** 499 (1976).
23. Wilson, J. M., *Surf. Sci.* **57,** 315 (1976).
24. Farias, M. H., Gellman, A. J., and Somorjai, G. A., *Surf. Sci.* **140,** 181 (1984).